Synthesis, Electronic Properties, and Solid-State Structure of $\{[(tpy)(Me_2bpy)Tc]_2(\mu\text{-}O)\}^{4+/2+}$

Joseph Barrera* and Jeffrey C. Bryan†

Materials and Chemical Design, CST-10, Los Alamos National Laboratory, Los Alamos, New Mexico 87545

Received June 1, 1995[⊗]

The oxo-bridged technetium(III) polypyridyl complex, $[(tpy)(Me_2bpy)Tc-O-Tc(tpy)(Me_2bpy)](OTf)_4$ **1**, abbreviated $[(N_5Tc)_2O]^{4+}$, was prepared from the reaction of $TcCl_3(tpy)$, TlOTf, and adventitous water. In contrast to other known μ-oxo systems of technetium or ruthenium, the cyclic voltammetric data of $[(N_5Tc)_2O]^{4+}$ suggests a relatively weak metal−metal interaction, however the visible absorption spectrum and the apparent magnetic properties suggests that this interaction cannot be completely dismissed. Crystallographic data of **1**: triclinic, $P\bar{1}$, $a = 12.906(2)$ Å, $b = 14.320(4)$ Å, $c = 19.568(2)$ Å, $\alpha = 77.55(1)°$, $\beta = 72.13(1)°$, $\gamma = 76.83(2)°$, $V = 3308$ Å^3, $Z = 2$. The Tc−O bond lengths are 1.833(6) and 1.830(6) Å, and the Tc−O−Tc bond angle is 171.1(3)°. The zinc reduction of **1** results in the two electron reduced oxo-bridged dimer, $[(N_5Tc)_2O]^{2+}$. Both complexes exhibit intense, low energy bands in the visible region characteristic of μ-oxo compounds, and these bands are red shifted by approximately 5000 cm^{-1} in the reduced complex.

Binuclear, transition metal complexes that are connected through a bridging ligand(s) are usually divided into three distinct classes. These classes include systems with relatively strong, weak, or virtually no indication of electronic interactions between the metal centers.[1] Inspired by the intial reports of Taube,[2] Meyer's investigations of the physical and chemical properties of various binuclear ruthenium complexes has led to a greater understanding of metal−metal interactions.[3] For example, a comparison of the related complexes $[(bpy)_2ClRuORuCl(bpy)_2]^{2+}$,[3d] $[(NH_3)_5RuORu(NH_3)_5]^{4+}$,[3b] and $[(NH_3)_5Ru(pyz)Ru(NH_3)_5]^{4+}$ [2] have shown that the extent of the metal−metal interaction is dependent upon both the ligand environment and the bridging ligand. In the case of the bridging oxo complexes, strong metal−metal electronic interactions have led to unique chemical properties that are significantly different than the related monomeric complexes. In fact the past 2 decades have witnessed nearly 100 reports involving the catalytic oxidation chemistry of bipyridine, ruthenium oxo complexes.[3a]

Described in this report is the synthesis as well as the structural and electronic characterization of the μ-oxo complexes $\{[(tpy)(Me_2bpy)Tc]_2(\mu\text{-}O)\}^{4+/2+}$. Although a recent report by Clarke et al.[4] has described the chemistry of very similar technetium compounds, i.e. $[(bpy)_2XTc]_2(\mu\text{-}O)\}^{2+}$ (X = Cl, Br), a comparison of the electochemical data for the two systems is interestingly very different. The dramatic differences in the electronic properties of $\{[(tpy)(Me_2bpy)Tc]_2(\mu\text{-}O)\}^{4+}$ and the related technetium and ruthenium systems will be discussed. In addition, unlike other known bridging oxo metal systems both the $Tc^{III}-Tc^{III}$ complex and the two electron reduced $Tc^{II}-Tc^{II}$ complexes can be isolated and important spectral comparisons made.

Experimental Section

The ^{1}H spectra was recorded on a Bruker WM300 NMR. Electrochemical experiments were performed in a helium-filled Vacuum Atmospheres glovebox using a PAR Model 362 potentiostat. Cyclic voltammograms were recorded (Kipp & Zonen BD90 XY recorder) in a standard three-electrode cell from +1.40 to −2.20 V vs NHE; $FeCp_2^{0/+} = 0.55$ V, with a glassy carbon working electrode. Elemental analysis was performed on a Perkin-Elmer PE-2400 Series II CHN analyzer. UV−visible spectra (Table 1) were recorded in acetonitrile on a Perkin Elmer Lambda-19. Infrared spectra were recorded as Nujol mulls on a Digilab FTS-40 spectrometer.

Materials. 2,2′,2″-Terpyridine (tpy), 4,4′-dimethylbipyridine (Me_2-bpy), and anhydrous *N*,*N*-dimethylacetamide (DMAc) were supplied from Aldrich and used as received. TlOTf was prepared from the addition of OEt_2 to dissolved Tl_2CO_3 in neat HOTf. 1,2-Dimethoxyethane was distilled from Na under nitrogen. Acetone supplied from Fluka was used as received. All other solvents were dried according to known procedures.

X-ray Structure Determination for $\{[(tpy)(Me_2bpy)]Tc]_2(\mu\text{-}O)\}(OTf)_4\cdot Me_2CO$. A deep red-purple prism, measuring 0.22 × 0.33 × 0.20 mm, was mounted on a glass fiber. Cell constants and an orientation matrix were obtained by least-squares refinement, using the setting angles of 25 reflections. Good crystal quality was also suggested by measuring ω scans of several intense reflections. Intensity data were obtained using $\theta-2\theta$ scans on an Enraf Nonius CAD4 diffractometer. A total of 14 334 reflections ($4 \le 2\theta \le 50°$, $\pm h$, $\pm k$, $\pm l$) were collected. The data were scaled for linear decay. No absorption correction was applied because of the low absorption coefficient (6.5 cm^{-1}) and good crystal shape. The data were averaged over $\bar{1}$ symmetry ($R_{int} = 4.4\%$). The structure was solved using direct methods and refined with full-matrix least-squares methods. All non-hydrogen atoms in $[(tpy)(Me_2bpy)]Tc]_2(\mu\text{-}O)^{4+}$, as well as atoms S(1), S(2), and S(3), were refined anisotropically. Hydrogen atom positions were calculated (C−H = 0.96 Å) and added to the structure factor calculations without refinement. Only the 7763 independent reflections with $F > 4\sigma_F$ were used in the refinement. All calculations were performed using SHELXTL PLUS (VMS) programs provided by Siemens Analytical. One of the four triflate anions exhibits complex disorder. Crystallographic data are given in Table 2, selected bond lengths and angles

† Current Address: Chemical Separations Group, MS-6119, Bldg. 4500S, Oak Ridge National Laboratory, Oak Ridge, TN 37831-6119.

⊗ Abstract published in *Advance ACS Abstracts,* March 15, 1996.

(1) Robin, M. B.; Day, P. *Adv. Inorg. Chem. Radiochem.* **1967**, *10*, 247.
(2) Creutz, C.; Taube, H. *J. Am. Chem. Soc.* **1973**, *95*, 1086.
(3) (a) Doppelt, P.; Meyer, T. J. *Inorg. Chem.* **1987**, *26*, 2027 and references therein. (b) Baumann, J. A.; Meyer, T. J. *Inorg. Chem.* **1980**, *19*, 345. (c) Callahan, R. W.; Keene, F. R.; Meyer, T. J.; Salmon, D. J. *J. Am. Chem. Soc.* **1977**, *99*, 1064. (d) Weaver, T. R.; Meyer, T. J.; Adeyemi, S. A.; Brown, G. M.; Eckberg, R. P.; Hatfield, W. H.; Johnson, E. C.; Muyyay, R. W.; Untereker, D. *J. Am. Chem. Soc.* **1975**, *97*, 3039.
(4) Lu, J.; Hiller, C. D.; Clarke, M. J. *Inorg. Chem.* **1993**, *32*, 1417.

0020-1669/96/1335-1825$12.00/0

Table 1. Electronic Spectral Data of Tc/Ru μ-Oxo Complexes[a]

complex	λ_{max}, nm (cm^{-1})	ϵ, M^{-1} cm^{-1}
$\{[(Me_2bpy)(tpy)Tc]_2O\}^{4+}$	744 (13 440)	1 184
	543 (18 400)	19 940
	468 (21 350)	13 510
	376 (26 850)	16 180
	284 (35 200)	54 150
$\{[(Me_2bpy)(tpy)Tc]_2O\}^{2+}$	751 (13 310)	12 670
	621 (16 100)	9 200
	406 (24 600)	9 150
	293 (34 130)	24 500
	234	28 700
$\{[(bpy)_2ClRu]_2O\}^{2+}$ [2d]	672 (14 880)	17 900
	289 (34 600)	39 000
	244	65 900
$\{[(bpy)_2ClRu]_2O\}^{3+}$	470 (21 280)	19 700
	300 (33 330)	46 000
	246	42 000
$\{[(NH_3)_5Ru]_2O\}^{4+}$ [2b]	503 (19 880)	16 230
	386 (25 900)	5 430
$\{[(NH_3)_5Ru]_2O\}^{5+}$ [b]	616 (16 230)	271
	342 (29 240)	25 280
	255 (39 220)	2 100

[a] All spectra were recorded in acetonitrile except where noted. [b] Recorded in H_2O.

Table 2. Summary of Crystallographic Data

complex	$\{[(tpy)(Me_2bpy)]Tc]_2(\mu\text{-}O)\}(OTf)_4\cdot Me_2CO$	Z	2
		fw	1703.2
chem formula	$C_{61}H_{52}F_{12}N_{10}O_{14}S_4Tc_2$	space group	$P\bar{1}$ (No. 2)
a, Å	12.907(2)	T, °C	−85
b, Å	14.320(4)	λ, Å	0.710 73
c, Å	19.568(2)	ρ_{calcd}, g cm^{-3}	1.71
α, deg	77.550(10)	μ, cm^{-1}	6.5
β, deg	72.130(10)	R[a]	0.066
γ, deg	76.83(2)	R_w[b]	0.096
V, Å^3	3308		

[a] $R = \sum||F_o| - |F_c||/\sum|F_o|$. [b] $R_w = [\sum w(|F_o| - |F_c|)^2/\sum w(F_o)^2]^{1/2}$.

Table 3. Selected Bond Lengths (Å) and Angles (deg) for $\{[(tpy)(Me_2bpy)]Tc]_2(\mu\text{-}O)\}(OTf)_4\cdot Me_2CO$

Tc(1)−O(1)	1.833(6)	Tc(2)−O(1)	1.830(6)
Tc(1)−N(1)	2.138(6)	Tc(2)−N(6)	2.121(6)
Tc(1)−N(2)	2.139(7)	Tc(2)−N(7)	2.132(8)
Tc(1)−N(3)	2.130(7)	Tc(2)−N(8)	2.136(6)
Tc(1)−N(4)	2.009(6)	Tc(2)−N(9)	2.006(7)
Tc(1)−N(5)	2.097(7)	Tc(2)−N(10)	2.127(6)
O(1)−Tc(1)−N(1)	98.0(2)	O(1)−Tc(2)−N(7)	173.3(2)
O(1)−Tc(1)−N(2)	174.1(2)	N(6)−Tc(2)−N(7)	75.7(3)
N(1)−Tc(1)−N(2)	76.1(2)	O(1)−Tc(2)−N(8)	93.7(3)
O(1)−Tc(1)−N(3)	90.7(3)	N(6)−Tc(2)−N(8)	97.3(2)
N(1)−Tc(1)−N(3)	101.8(2)	N(7)−Tc(2)−N(8)	87.9(3)
N(2)−Tc(1)−N(3)	90.0(3)	O(1)−Tc(2)−N(9)	94.4(3)
O(1)−Tc(1)−N(4)	92.8(2)	N(6)−Tc(2)−N(9)	167.5(3)
N(1)−Tc(1)−N(4)	169.2(3)	N(7)−Tc(2)−N(9)	92.3(3)
N(2)−Tc(1)−N(4)	93.1(3)	N(8)−Tc(2)−N(9)	78.5(3)
N(3)−Tc(1)−N(4)	77.8(3)	O(1)−Tc(2)−N(10)	93.8(3)
O(1)−Tc(1)−N(5)	97.0(3)	N(6)−Tc(2)−N(10)	104.6(2)
N(1)−Tc(1)−N(5)	99.8(3)	N(7)−Tc(2)−N(10)	87.3(3)
N(2)−Tc(1)−N(5)	84.7(3)	N(8)−Tc(2)−N(10)	155.6(3)
N(3)−Tc(1)−N(5)	155.8(2)	N(9)−Tc(2)−N(10)	77.8(3)
N(4)−Tc(1)−N(5)	78.9(3)	Tc(1)−O(1)−Tc(2)	171.1(3)
O(1)−Tc(2)−N(6)	97.6(3)		

in Table 3, and selected atomic coordinates in Table 4. Complete tabulations of crystallographic data, bond lengths and angles, atomic coordinates, thermal parameters, and a completely labeled ball and stick diagram are available as Supporting Information.

$\{[(tpy)(Me_2bpy)]Tc]_2(\mu\text{-}O)\}(OTf)_4$. $TcCl_3(tpy)$ (0.275 g, 0.63 mmol), Me_2bpy (0.165 g, 0.89 mmol), and TlOTf (0.461 g, 1.30 mmol) were placed in a vial and suspended in DMAc (8 mL), DME (2 mL), and toluene (1 mL). The reaction mixture was stirred for 46 h at 65 °C. The reaction mixture was filtered through Celite which resulted in a red-burgandy colored filtrate and a dark gray-green solid. The filtrate was added dropwise to a stirring OEt_2 (80 mL) and CH_2Cl_2 (15 mL) solution. After 30 min the solution was decanted from the red-purple oil, and the latter dissolved in wet acetone (addition of two Pasteur pipet drops of water to 8 mL of acetone). The solution was stirred at 45 °C for 5 h during which time a white-gray precipitate formed and the color of the solution turned from red-burgandy to purple. The reaction mixture was filtered through Celite, and the acetone reduced to half volume under vacuum. Upon slow addition of OEt_2 a precipitate formed, and the reaction mixture stirred for 1 h. The suspension was filtered, and the resulting solid was washed with OEt_2 (2 × 1 mL), 0.237 g, 45%. X-ray quality crystals were obtained from a cooled (−40 °C) acetone/OEt_2 solution. ^{1}H NMR (acetone-d_6): 8.87 (m, 7H), 8.76 (m, 2H), 8.66 (m, 7H), 8.51 (t, 4H), 8.37 (s, 2H), 7.83 (t, 3H), 7.72 (d, 2H), 7.17 (m, 3H), 6.91 (d, 2H), 6.82 (d, 2H), 2.78 (s, 6H), 2.25 (s, 6H). CV (DMAc; TBAH; 100 mV s^{-1}): $E_{p,c} = 1.24$ V, $E_{1/2} = -0.14$ V, $E_{1/2} = -0.39$ V, $E_{p,a} = -1.08$ V vs NHE. Anal. Calcd for $Tc_2C_{61}H_{52}N_{10}O_{14}S_4F_{12}$ (formula based upon X-ray analysis): C, 43.06; H, 3.08; N, 8.23. Found: C, 43.41; H, 3.38; N, 7.81.

$\{[(tpy)(Me_2bpy)]Tc]_2(\mu\text{-}O)\}(OTf)_2$. $\{[(tpy)(Me_2bpy)]Tc]_2(\mu\text{-}O)\}(OTf)_4$ (0.154 g, 0.09 mmol) was dissolved in acetone (12 mL), and Zn powder added (0.45 g). The reaction was stirred for 1 h at room temperature. During this time the reaction solution changes color from purple to blue-green. The reaction mixture was filtered through Celite, and the collected solids washed with acetone (4 × 2 mL). The solids were than extracted with MeCN (4 × 2 mL) and the extracts filtered through Celite. Upon the slow addition of OEt_2 a precipitate formed, and the reaction mixture was stirred for 1 h. The suspension was filtered and the resulting solid was washed with OEt_2; yield 0.052 g, 82%. ^{1}H NMR(CD_3CN): 8.80 (br s, 2H), 8.36 (br s, 2H), 7.92 (br s, 4H), 7.49 (br s, 2H), 7.30 (br s, 5H), 7.09 (m, 2H), 6.85 (br s, 2H), 6.61 (br s, 9H), 6.20 (br s, 6H), 2.66 (br s, 6H), 2.53 (br s, 6H). CV (DMAc; TBAH; 100 mV s^{-1}): $E_{p,c} = 1.24$ V, $E_{1/2} = -0.14$ V, $E_{1/2} = -0.39$ V, $E_{p,a} = -1.08$ V vs NHE. Anal. Calcd for $Tc_2C_{56}H_{46}N_{10}O_7S_2F_6$: C, 50.0; H, 3.45; N, 10.41. Found: C, 50.28; H, 3.38; N, 10.19.

Table 4. Selected Coordinates (×10^4) for $\{[(tpy)(Me_2bpy)]Tc]_2(\mu\text{-}O)\}(OTf)_4\cdot(Me_2CO$

	x	y	z	U_{eq}[a]
Tc(1)	2049(1)	1895(1)	3388(1)	16(1)
Tc(2)	1636(1)	1817(1)	1638(1)	16(1)
O(1)	1840(4)	1957(3)	2493(3)	15(2)
N(1)	637(5)	2935(4)	3799(3)	17(2)
N(2)	2132(5)	1919(5)	4459(3)	19(2)
N(3)	1414(5)	572(5)	3769(3)	20(2)
N(4)	3428(5)	892(4)	3185(3)	18(2)
N(5)	3271(5)	2769(5)	3047(3)	20(2)
N(6)	2870(5)	2594(5)	923(3)	19(2)
N(7)	1535(5)	1765(5)	580(4)	20(2)
N(8)	2619(6)	398(5)	1628(3)	24(3)
N(9)	483(6)	974(5)	2118(3)	24(3)
N(10)	145(6)	2850(5)	1752(4)	23(3)
S(1)	6085(2)	6394(2)	2542(1)	27(1)
S(2)	1306(2)	6276(2)	2948(1)	29(1)
S(3)	6595(2)	1291(2)	4437(2)	47(1)
S(4)	7476(4)	899(4)	989(3)	37(1)
S(4A)	7582(5)	1367(5)	660(3)	50(1)

[a] Equivalent isotropic U_{eq} defined as one third of the trace of the orthogonalized $\mathbf{U}_{ij}$ tensor and given in units of Å^2 × 10^3.

Results

Oxo-bridged binuclear complexes have been reported for most of the transition metals including that of technetium.[4,5] In general, these complexes are prepared from metal−oxo[2,4] or metal−aquo[3] complexes if a second or third row metal is involved or from metal−hydroxo complexes in the case of a first row metal.[6] During our investigation involving the substitution chemistry of various L_nTc^{III} complexes, $\{[(tpy)(Me_2bpy)Tc]_2\mu\text{-}O\}(OTf)_4$, **1** [abbreviated $[(N_5Tc)_2O]^{4+}$], was prepared from $TcCl_3(tpy)$, Me_2bpy, and TlOTf in the presence of

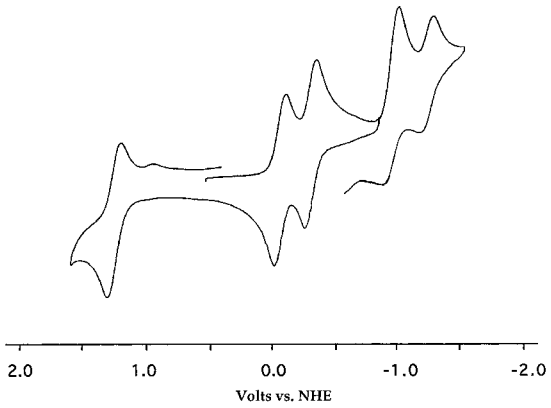

Figure 1. Cyclic voltammogram of {[(tpy)(Me$_2$bpy)Tc]$_2$(μ-O)}$^{4+}$ in DMAc (TBAH), 100 mV/s.

adventitous water. The preparation of $[(N_5Tc)_2O]^{4+}$ is apparently more complicated than the apparent hydrolysis of [TcCl(tpy)(Mebpy)]$^{2+}$, since electrochemical data of the precipitated initial oily residue suggests a mixture of at least three different substitution products prior to the addition of "wet" acetone (see Experimental Section). However, after 5 h at 45 °C only the oxo-bridged complex is observed in the cyclic voltammogram. The ^{1}H NMR of $[(N_5Tc)_2O]^{4+}$ exhibits a diamagnetic spectrum with the aromatic hydrogens between 8.9 and 6.8 ppm, and the methyl hydrogens of the 4-substituted bipyridine at 2.78 and 2.25 ppm. Although octahedral complexes of Tc^{III} usually exhibit a Knight-shifted ^{1}H NMR, the apparent dimagnetism of **1** is not so surprising. The observed room tempertaure magnetic properties may be rationalized in terms of a spin−spin exchange interaction through the bridging oxo ligand or a HOMO description that includes the two metal centers and the bridging oxo ligand (*vide infra*).[3d,7]

The addition of Zn powder to an acetone solution of $[(N_5Tc)_2O]^{4+}$ results in the formation of the corresponding d^5-d^5, $Tc^{II}-Tc^{II}$, oxo-bridged dimer, [(tpy)(Me$_2$bpy)Tc2](OTf)$_2$, **2** {abbreviated $[(N_5Tc)_2O]^{2+}$}. This species exhibits identical electrochemical data to $[(N_5Tc)_2O]^{4+}$ with the exception that zero current is now observed on the reduced side of the two reversible couples, Figure 1. Similar to that of **1** the ^{1}H NMR spectrum of **2** exhibits a ^{1}H NMR spectrum with resonances between 1 and 10 ppm; however, the resonances are relatively broad. The aromatic hydrogens exhibit resonances between 9.0 and 6.0 ppm, and the methyl hydrogens, at 2.66 and 2.53 ppm.

Addition of $^{18}OH_2$ to the acetone solution results in the ^{18}O-labeled compound, $[(N_5Tc)_2{}^{18}O]^{4+}$. This complex exhibits a weak absorption at 864 cm^{-1} (Nujol, calculated, 848 cm^{-1}), which is shifted 29 cm^{-1} to lower energy than the parent complex, i.e. 893 cm^{-1}. With the exception of the strong absorption band at 781 cm^{-1}, no other significant spectral differences between the two IR spectra were observed in the range 500−1000 cm^{-1}. The IR spectrum of $[(N_5Tc)_2O]^{2+}$ is similar to that of $[(N_5Tc)_2O]^{4+}$, with the exceptions that the absorption peak at 893 cm^{-1} is absent and a weak absorption peak of similar intensity is now observed at considerably lower energy, i.e. 546 cm^{-1}. The relatively strong absorption at 781 cm^{-1} observed in $[(N_5Tc)_2O]^{4+}$ also needs to be mentioned since this peak shifts to lower energy in both the ^{18}O-labeled compound, i.e. 774 cm^{-1} (calc. 742 cm^{-1}), and $[(N_5Tc)_2O]^{2+}$, i.e. 746 cm^{-1}.

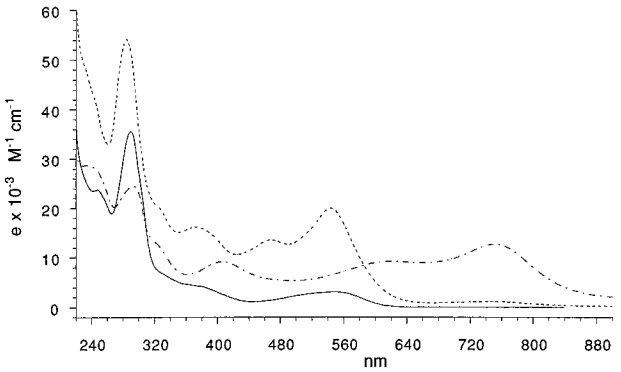

Figure 2. UV−visible spectra in acetonitrile: (a) $[(N_5Tc)_2O]^{4+}$ (dash), (b) $[(N_5Tc)_2O]^{4+}$ (dash−dot), (c) $[TcCl_2(Me2bpy)_2]^+$ (solid).

The cyclic voltammetric data also indicates the binuclear nature of $[(N_5Tc)_2O]^{4+}$, since a pair of one electron, reversible, reduction couples seperated by 250 mV, i.e. −0.14 and −0.39 V, is observed, Figure 1. In addition, a one electron, semireversible oxidation at 1.24 V, and a one electron, irreversible reduction at −1.08 V is observed.[8]

The UV−visible spectra of **1** and **2** are shown in Figure 2. In addition, the spectrum of the mononuclear complex, [TcCl$_2$(Me$_2$bpy](OTf), is shown for comparative purposes. The absorption spectrum of $[(N_5Tc)_2O]^{4+}$ is relatively complex with several absorption maxima between 300 and 600 nm. Analogous to the ruthenium oxo-bridged compounds,[3b,d] a strong, low energy band (i.e. λ_{max}, 543 nm; ϵ, 20 000 M^{-1} cm^{-1}) is observed, Table 1. In addition, there exist three other intense bands in the visible region that appear to be present in the ruthenium case but are not clearly resolved in the latter. A relatively weak, very broad band (i.e. λ_{max}, 744 nm; ϵ, 1200 M^{-1} cm^{-1}) is also observed. In the UV region typical $\pi-\pi^*$ transitions from the polypyridyl ligands are observed: a sharp, intense band at λ_{max} 284 nm; (ϵ 54 200 M^{-1} cm^{-1}) and two unresolved transitions between 220 and 240 nm. The absorption spectrum of $[(N_5Tc)_2O]^{2+}$ is very similar in shape to that of $[(N_5Tc)_2O]^{4+}$, with the exception that the two low energy bands are red shifted by approximately 5000 cm^{-1}. A slight red shift is also observed in the UV region of the spectrum. For example the sharp, intense $\pi-\pi^*$ transition (i.e. λ_{max}, 293 nm; ϵ, 24 500 M^{-1} cm^{-1}) is shifted by 1070 cm^{-1}.

Solid-State Structure. The solid-state structure of $[(N_5Tc)_2O]^{4+}$, illustrated in Figure 3, clearly establishes the binuclear nature of **1**. Each technetium atom is surrounded by a distorted octahedron of donor atoms, made up of five nitrogen atoms from the aromatic amine ligands and one oxygen atom from the oxo bridge. The distortions are probably a result of the small bite angles of both the bipyridine and terpyridine ligands, i.e. 76 and 156°, respectively. The cation has approximate 2-fold (noncrystallographic) symmetry which relates the two

(5) (a) Clarke, M. J.; Kastner, M. E.; Podbielski, l. A.; Fackler, P. H.; Schreifels, J.; Meinken, G.; Srivastava, S. C. *J. Am. Chem. Soc.* **1988**, *110*, 1818. (b) Tisato, F.; Refosco, F.; Mazzi, U.; Bandoli, G.; Nicolini, M. *Inorg. Chim. Acta.* **1989**, *157*, 227; **1989**, *164*, 127. (d) Pilliai, M. R. A.; John, C. S.; Lo, J. M.; Schlemper, E. O.; Troutner, D. E. *Inorg. Chem.* **1990**, *29*, 1850. (e) Bandoli, G.; Nicolini, M.; Mazzi, U.; Refosco, F. *J. Chem. Soc., Dalton Trans.* **1984**, 2505. (f) Kastner, M. E.; Fackler, P. H.; Podbielski, L.; Charkoudian, J.; Clarke, M. J. *Inorg. Chim. Acta* **1986**, *114*, 11. (g) Baldas, J.; Colmanet, S. F.; Mackay, M. F. *J. Chem. Soc., Dalton Trans.* **1988**, 1725.
(6) Griffith, W. P. *Coord. Chem. Rev.* **1970**, *5*, 459.
(7) Schugar, H.; Rossman, G. R.; Barraclough, C. G.; Gray, H. B. *J. Am. Chem. Soc.* **1972**, *94*, 2683.

(8) Electrochemical reversibility was determined from the the peak separations (ΔEp), and the ratio of the anodic to cathodic peak currents ($i_{p,a}/i_{p,c}$) in the cyclic voltammograms. The two distinct $Tc^{III/II}$ couples exhibited a peak separation of approximately 80 mV and a peak ratio near unity. The ferrocene standard under identical cell conditions exhibited a peak separation of approximately 70 mV. The number of electrons for each redox couple were determined from a known amount of ferrocene and sample. The peak ratios were then measured as each peak was scanned.

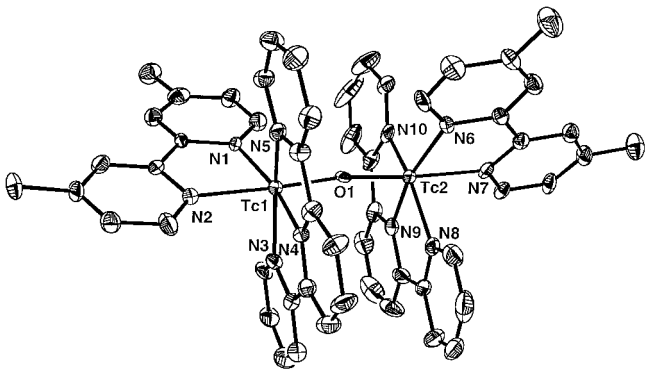

Figure 3. ORTEP drawing (50% probability ellipsoids) of $[(tpy)(Me_2bpy)]Tc]_2(\mu\text{-}O)^{4+}$. Hydrogen atoms are omitted for clarity.

"N_5Tc" fragments through the oxo bridge. The asymmetric unit also contains four triflate anions, one of which exhibits complex disorder, and one molecule of acetone (see Supporting Information).

The bond distances and angles in $[(N_5Tc)_2O]^{4+}$ are very similar to those reported by Clarke et al. for the closely related $[X(bpy)_2Tc]_2(\mu\text{-}O)^{2+}$ (X = Cl, Br) and $[Cl(phen)_2Tc]_2(\mu\text{-}O)^{2+}$ complexes.[4] The Tc(1)−O(1)−Tc(2) bond angle of 171.1(3)° in $[(N_5Tc)_2O]^{4+}$ is indistinguishable from Clarke's complexes, which exhibit an average value of 171(1)°.[4] However, this value is 14 and 6° greater than the observed Ru−O−Ru bond angle in $[(bpy)_2(X)Ru{-}O{-}Ru(X)(bpy)_2]^{n+}$; X = NO_2[9] and H_2O,[10] respectively. This increase can be attributed to greater π-bonding between Tc and the oxo bridge.[4] The bending at the oxo bridge allows stronger interaction between two of the three pyridine rings that lie parallel to each other on each terpyridyl ligand. These rings contain N(3) and N(4) on Tc(1) and N(8) and N(9) on Tc(2). The interplanar separation between these two sets of rings is approximately 3.4 Å, and the interplanar angle is roughly 6°. This separation is similar to values reported for purines[11a] and other aromatic molecules[11b] and suggests a favorable π-stacking interaction.

The bond distances of 1.833(6) and 1.830(6) Å for Tc(1)−O(1) and Tc(2)−O(1), respectively, are identical within experimental error. Similar M−O−M distances are observed in the other reported technetium systems,[4,5] and bond distances in the ruthenium system average 1.88 Å.[9,10]

The Tc−N(tpy) bond distances are similar to $[TcBr(tpy)(PMe_2Ph)_2]^{+}$ [12] with the interior nitrogen atom on average shorter than the two exterior nitrogen atoms by approximately 0.12 Å. The Tc−N(bpy) bond distances (2.13−2.14 Å) are similar to other Tc^{III} complexes.[4,13] As observed for the closely related $[X(bpy)_2Tc]_2(\mu\text{-}O)^{2+}$ (X = Cl, Br) $[Cl(phen)_2Tc]_2(\mu\text{-}O)^{2+}$ complexes,[4] no difference is observed between the Tc−N(bpy) bond distance trans to the oxo and the Tc−N(bpy) bond distance trans to the interior terpyridine nitrogen. The Tc−N(bpy) and the exterior Tc−N(tpy) distances are on average slightly longer than those observed in similar Ru^{III}−bipyridine systems.[9,10]

Crystalline material of $[(N_5Tc)_2O]^{2+}$ is obtained upon the vapor diffusion of OEt_2 into an acetone solution. Unfortunately, four distinct crystallizations resulted in very long and thin single crystals that resulted in a very weak intensity pattern. Attempts to utilize larger samples resulted in diffraction patterns characteristic of multiple distinct crystals.

Discussion. Polypyridyl, bridged complexes of ruthenium have been throughly investigated by the Meyer[3,10,14] group and others over the past 2 decades. Interestingly, the electronic properties of these binuclear systems have been shown to be dependant upon both the bridging ligand and the ligand environment. For example, the electronic properties of the bipyridine oxo-bridged complex are consistent with a strong electronic interaction between the two ruthenium ions, while the electronic properties of the analogous pyrazine bridge is consistent with a very weak metal−metal interaction. In addition, small electronic differences are observed between the pyrazine bridged bipyridine and ammine systems, i.e. the Creutz−Taube ion.

The electronic properties of the technetium polypyridyl oxo-bridged complex reported here are best described as having a relatively weak electronic interaction between the metal centers. This is in sharp contrast to the related ruthenium complexes $[(bpy)_2(X)Ru{-}O{-}Ru(X)(bpy)_2]^{n+}$ (X = NO_2[9] and H_2O)[10] and the technetium complex $[Cl(bpy)_2Tc]_2(\mu\text{-}O)^{2+}$.[4] The observed differences in the electronic and structural properties between these systems are discussed below.

IR Data. The absorption band at 893 cm^{-1} in the IR spectrum of $[(N_5Tc)_2O]^{4+}$ is tentatively assigned to the antisymmetric bending mode of M−O−M. This assignment is based upon the observed shift to lower energy in $[(N_5Tc)_2{}^{18}O]^{4+}$, and the reported IR data of other M−O−M complexes.[6] Previous reports[4,5] of Tc−O−Tc complexes have assigned absorptions between 625 and 730 cm^{-1} to this particular stretching mode. The absorption band at 781 cm^{-1} in the IR spectrum of $[(N_5Tc)_2O]^{4+}$ is also a strong candidate for υ_{as}(M−O−M) due to the observed shift to lower energy in both $[(N_5Tc)_2{}^{18}O]^{4+}$ and $[(N_5Tc)_2O]^{2+}$. The absorption band at 546 cm^{-1} in the two-electron reduced complex, $[(N_5Tc)_2O]^{2+}$, is more likely the result of a symmetrical Tc−O−Tc vibration mode. The expected increase in the bending of $[(N_5Tc)_2O]^{2+}$, relative to $[(N_5Tc)_2O]^{4+}$, can justify such a stretch becoming infrared active.[3b] To the best of our knowledge the complexes, $[(bpy)_2XRu{-}O{-}RuX(bpy)_2]^{2+}$ (X = Cl, NO_2, H_2O) and $[(NH_3)_5Ru{-}O{-}Ru(NH_3)_5]^{4+}$ are the only other examples of a second row, binuclear, transition metal compounds with an oxo-bridge and an electronic configuration of d^5−d^5. Unfortunately, definitive assignments to the antisymmetric stretches in the bipyridyl system could not be made due to the interference with strong bipyridine vibrations below 800 cm^{-1}. In the Ru amine system observed absorptions at 782 and 747 cm^{-1} were tentatively assigned as the asymmetric stretches for $[(NH_3)_5Ru{-}O{-}Ru(NH_3)_5]^{5+}$ and $[(NH_3)_5Ru{-}O{-}Ru(NH_3)_5]^{4+}$, respectively.[2]

Electrochemistry. The redox couples of $[(N_5Tc)_2O]^{4+}$ are in contrast to the complexes, $[Cl(pic)_4Tc{-}O{-}TcCl_4(pic)]$ and $[Cl(bpy)_2Tc{-}O{-}Tc(bpy)_2Cl]^{2+}$, reported by Clarke.[4,5a] The pyridine complex exhibits a one-electron, electrochemically reversible oxidation and reduction couple separated by 1.5 V, and the bipyridine complex exhibits two reversible oxidation couples separated by 0.67 V. These values strongly suggest that the two metals in these systems are strongly coupled and that an odd electron would essentially be delocalized on both metal centers. Electrochemical oxidation of $[(bpy)_2ClRu{-}O{-}$

(9) Phelps, D. W.; Kahn, E. M., Hodgson, D. J. *Inorg. Chem.* **1975**, **14**, 2486.
(10) Gilbert, J. A.; Eggleston, D. S.; Murphy, W. R.; Geselowitz, D. A.; Gersten, S. W.; Hodgson, D. J.; Meyer, T. J. *J. Am. Chem. Soc.* **1985**, *107*, 3855.
(11) (a) Bugg, C. E. *Jerusalem Symp. Quantum Chem. Biochem.* **1972**, *4*, 178. (b) Herbstein, F. H. *Perspect. Struct. Chem.* **1971**, *4*, 166.
(12) Wilcox, B. E.; Ho, D. M.; Deutsch, E. *Inorg. Chem.* **1989**, *28*, 3917.
(13) (a) Breikss, A. I.; Nicholson, T.; Jones, A. G.; Davison, A. *Inorg, Chem.* **1990**, *29*, 640. (b) Wilcox, B. E.; Ho, D. M.; Deutsch, E. *Inorg. Chem.* **1989**, *28*, 1743.
(14) (a) Dobson, J. C.; Sullivan, B. P.; Doppelt, P.; Meyer, T. J. *Inorg. Chem.* **1988**, *27*, 3863. (c) Johnson, E. C.; Sullivan, B. P.; Salmon, D. J.; Adeyemi, S. A.; Meyer, T. J. *Inorg. Chem.* **1978**, *17*, 2211.

Table 5. Electrochemical Potentials of Structurally Related Complexes[a]

$$M^{d^3}-M^{d^3} \overset{E_1}{\rightleftharpoons} M^{d^3}-M^{d^4} \overset{E_2}{\rightleftharpoons} M^{d^4}-M^{d^4} \overset{E_3}{\rightleftharpoons} M^{d^4}-M^{d^5} \overset{E_4}{\rightleftharpoons} M^{d^5}-M^{d^5} \overset{E_5}{\rightleftharpoons} M^{d^5}-M^{d^6}$$

complex	E_1	E_2	E_3	E_5	E_5	K_{com}
{[(bpy)(tpy)Tc]$_2$O}$^{n+}$		1.24[b]	−0.14	−0.39	−1.08[c]	10^4
{[Cl(bpy)$_2$Tc]$_2$O}$^{n+}$	1.48	0.81	−0.58			10^{11}
{[Cl(bpy)$_2$Ru]$_2$O}$^{n+}$			2.18	0.95	−0.15	10^{20}
{TcCl$_2$(bpy)}$^+$		$Tc^{IV/III}$	$Tc^{III/II}$		$Tc^{II/I}$	
		1.13	−0.16		−1.11	

[a] Potentials are reported vs NHE, $FeCp_2^{0/+}$ = 0.55 V, SSCE = 0.28 V. [b] Semireversible oxidation (100 mV/s). [c] Irreversible reduction.

RuCl(bpy)$_2$]$^{2+}$ (d^5-d^5) consists of two, reversible, one-electron oxidations separated by 1.23 V, i.e. 0.95 and 2.18 V, respectively. Similar electrochemical behavior was also reported for [(bpy)$_2$(NO$_2$)Ru−O−Ru(NO$_2$)(bpy)$_2$]$^{2+}$,[3d] and [(NH$_3$)$_5$Ru−O−Ru(NH$_3$)$_5$].[3b] The latter ammine complex, ΔE = 1.35 V, suggests a slightly stronger metal−metal interaction than the similar bipyridine complex. In addition, the electrochemical properties of these Ru oxo-bridged dimers are quite different than the properties of their mononuclear analog, [RuCl$_2$(bpy)$_2$]$^+$. The latter exhibits a reversible, one electron oxidation that is 1.30 V more positive than the initial oxidation for the dimer. Thus, the electrochemical data of the Ru oxo-bridged dimers are consistent with an oxidation from a delocalized molecular orbital generating two Ru ions with a formal charge of 3.5. An electrochemical summary of the systems is provided in Table 5.

In contrast the electrochemical properties of [(bpy)$_2$ClRu−pyz−RuCl(bpy)$_2$]$^{2+}$ (d^6-d^6); pyz = pyrazine, and the Creutz-Taube ion, i.e. [(NH$_3$)$_5$Ru−pyz−Ru(NH$_3$)$_5$]$^{5+}$ (d^6-d^5) exhibit a separation in redox potentials of 0.12 and 0.37 V, respectively. Accordingly, these complexes are considered to be weakly coupled systems.[3c] The small electronic differences of these two systems was explained in terms of the availability of π-back-bonding in the bipyridyl complex. Consequently, the resulting decrease in electron density at the metal centers may account for the apparent decrease in the electronic delocalization between the metal centers.[3c]

In the case of [(N$_5$Tc)$_2$O]$^{4+}$, the two, reversible, one electron electrochemical reductions, i.e. d^4-d^4 to d^5-d^5, are separated by 0.25 V. This observation strongly suggests that unlike either the previously reported technetium or ruthenium oxo-bridged systems, the two Tc ions are *not* strongly coupled to each other. Thus the reductions occur in molecular orbitals which are significantly localized on each technetium center. To the best of our knowledge, such electrochemical behavior is unprecedented in oxo-bridged systems involving a second or third row transition metal. In fact, Meyer's initial interest in oxo-bridged complexes was to develop a system in which strong metal−metal interactions existed through a "short bridging distance with the possibility of strong π-overlap". Also, the redox potentials of [(N$_5$Tc)$_2$O]$^{4+}$ are very similar in magnitude to those of the related mononuclear complex, [TcCl$_2$(Me$_2$bpy)]$^+$. The latter exhibits two reversible reductions at −0.16 and +1.11 V, and a reversible oxidation at 1.13 V. In contrast to the Ru−oxo system, these values are nearly identical to that of the dimer and thus consistent with a relatively weak metal−metal interaction.

The origin of the unusually weak metal−metal interaction in this system, as suggested by the electrochemical data, is best explained by the presence of unusually strong π-interactions between the bipyridine ligands and the reduced, electron-rich metal centers. A recent study of low-valent technetium pyridyl complexes indicate the existence of these unusually strong π-interactions by significant decreases in metal nitrogen bond distances and extraordinary differences in the absorption spectra in identical Tc^{III} and Tc^{II} complexes.[15]

The observation in the solid-state structure that the axial bipyridine ligands are normal to each other also suggests that metal to bipyridine π-interactions play an important role in the electronic character of **1** as well as the other reported Tc and Ru systems. In this orientation the LUMO's in **1**, π_1* and π_2*, would be significantly stabilized by the empty π* orbitals of the axial bipyridine ligands. The decrease in the absolute energies of these orbitals accounts for the relatively positive reduction potentials, the observed red shift in the electronic spectrum upon reduction (*vide infra*), and the stability of the d^5-d^5 dimer.

UV−Visible Spectra. The UV−visible spectra of [(N$_5$Tc)$_2$O]$^{4+}$ and [(N$_5$Tc)$_2$O]$^{2+}$ are very similar to that of the known technetium and ruthenium oxo-bridged complexes. Both **1** and **2** exhibit the intense, low energy bands characteristic of oxo-bridged complexes. Also, the UV−visible spectrum of [(N$_5$Tc)$_2$O]$^{4+}$ mirrors that of the other systems in that the band at 468 nm is considerably red shifted i.e. to 621 nm, ΔE = 5250 cm^{-1}, in the two-electron reduced Tc complex [(N$_5$Tc)$_2$O]$^{2+}$. For comparison, [(bpy)$_2$ClRu−O−RuCl(bpy)$_2$]$^{3+/2+}$ and [(NH$_3$)$_5$Ru−O−Ru(NH$_3$)$_5$]$^{5+/4+}$ exhibit red shifts of 6400 and 9400 cm^{-1} upon a one-electron reduction, respectively.[3b,d] In the case of the bipyridine ruthenium systems these low enregy, intense absorptions were assigned as a transition from a π^b orbital(s) to the antibonding orbitals π^*_1 and π^*_2, Figure 3. This molecular orbital scheme is identical to that proposed by Meyer's.[3d] The absolute energies of these transitions in [(N$_5$Tc)$_2$O]$^{4+}$ and [(N$_5$Tc)$_2$O]$^{2+}$ are nearly identical in energy to the transitions observed in the corresponding oxidized and reduced forms of [(bpy)$_2$ClRu−O−RuCl(bpy)$_2$]$^{3+/2+}$. In addition, the red shift of approximately 5000 cm^{-1} between [(N$_5$Tc)$_2$O]$^{4+}$ and [(N$_5$Tc)$_2$O]$^{2+}$ suggests that both π_1* and π_2* are substantially destabilized in the oxidized complex. Such a shift is consistent with [(N$_5$Tc)$_2$O]$^{4+}$ having a stronger Tc−O−Tc orbital interaction than [(N$_5$Tc)$_2$O]$^{2+}$ which is to be expected since the additional two electrons in the latter are localized in antibonding orbital combinations of Tc−O−Tc. This should also result in a decrease of the Tc−O−Tc bond angle, and thus further reduce this orbital interaction in [(N$_5$Tc)$_2$O]$^{2+}$.

In comparison to the ruthenium systems, the technetium dimers also exhibit a second intense absorption to lower energy that also exhibits a red shift, i.e. from 543 to 751 nm, of approximately 5000 cm^{-1} upon reduction. These absorptions are approximately 3000 cm^{-1} lower in energy than the absorptions described above, and thus most likely arise from a combination of transitions between the relatively nonbonding d_{xy} orbitals and the slightly destabilized π_1^n and π_2^n orbitals to the antibonding orbitals π_1* and π_2*.

The apparent magnetism in both [(N$_5$Tc)$_2$O]$^{4+/2+}$ can be explained by either the molecular orbital scheme, Figure 4, or a superexchange spin−spin coupling mechanism. The latter mechanism would result in a singlet and triplet state separated by 2J and has been used to explain the magnetic properties of oxo-bridged Fe^{III} complexes.[5] Although magnetic measurements were not investigated for [(N$_5$Tc)$_2$O]$^{4+/2+}$, the molecular orbital treatment best explains the apparent diamagnetism of [(N$_5$Tc)$_2$O]$^{4+}$ and the near diamagnetism of [(N$_5$Tc)$_2$O]$^{2+}$. In the case of the $Tc^{III}-Tc^{III}$ dimer the diamagnetic room temperature ^{1}H NMR is easily explained in terms of the highly

(15) Barrera, J.; Burrell, A. K.; Bryan, J. C. *Inorg. Chem.* **1996**, *35*, 335.

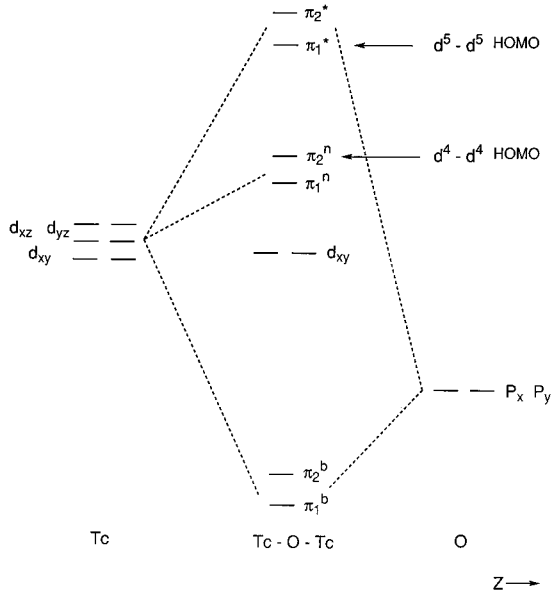

Figure 4. Molecular orbital description of Tc−O−Tc.

destabilized LUMO's, π_1^* and π_2^*, and in the case of the Tc^{II}−Tc^{II} dimer the apparent slight paramagnetism is easily explained in terms of a singlet ground state (π_1^{*2}), and a low lying triplet state ($\pi_1^*\pi_2^*$). The π_1^* and π_2^* orbitals are expected to be nondegenerate because of the low symmetry of the technetium centers resulting from the bend of Tc−O−Tc bridge. A d^5−d^5 spin exchange mechanism however should not be ruled out in the case of $[(N_5Tc)_2O]^{2+}$, since the Tc−O−Tc orbital interactions are expected to be much weaker.

Conclusions. The electronic properties of the technetium oxo-bridged complexes, $[(N_5Tc)_2O]^{4+}$ and $[(N_5Tc)_2O]^{2+}$, are quite unique when compared to very similar complexes of ruthenium and technetium. The electrochemical properties of the latter, i.e. the significant differences in the redox potentials between the dimer and analogous mononuclear complexes as well as the large separation in the redox potentials of the reduced and oxidized complexes, are consistent with the existence of a strong, chemically significant interaction between the metal ions through the bridging oxide ligand. That is electrochemical oxidation occurs from a molecular orbital that is significantly *delocalized* over both metal centers. In contrast the electrochemical properties of $[(N_5Tc)_2O]^{4+}$, i.e. nearly identical redox potentials with analogous mononuclear complexes as well as a difference of only 0.25 V between the 2^+ and 3^+ ions, suggest a relatively weak metal−metal interaction. Thus, electrochemical oxidation occurs from molecular orbitals that are significantly *localized* on each metal center. On the other hand, the two metal systems both exhibit intense, low energy electronic transitions characteristic of bridging oxo complexes. This as well as the dramatic red shift of these transitions upon reduction suggests that electronically both systems can be described by a *delocalized* molecular orbital scheme. Thus, $[(N_5Tc)_2O]^{4+}$ is a unique oxo bridged system that possesses both localized and delocalized electronic properties. As such this system poses an interesting dilemma for theoreticians who must wage a battle between an MO calculation that would favor a delocalized description and a valence bond calculation that would favor a more localized description.

Acknowledgment. This work was supported by the Laboratory Directed Research and Development Program at Los Alamos National Laboratory. The authors would also like to thank Dr. Robert Hightower (Oak Ridge National Laboratory) for a generous gift of ammonium pertechnetate.

Supporting Information Available: Complete tabulations of crystallographic data, bond lengths and angles, atomic coordinates, and thermal parameters, and completely labeled diagrams for {[(tpy)(Me_2-bpy)]Tc]$_2$(μ-O)}$(OTf)_4$·Me_2CO (11 pages). This material is contained in many libraries on microfiche, immediately follows this article in the microfilm version of the journal, and can be ordered from the ACS; see any current masthead page for ordering information.

IC950671B